This copy of the ESI replaces the previous version published on 30/09/2021

Supplementary Information to Influence of the PO_uN_{4-u} structural units on the formation energies and transport properties of lithium phosphorus oxynitride: A DFT study

Pascal Henkel[a,b], Jürgen Janek[a,b] and Doreen Mollenhauer[a,b,#]

[a] Institute of Physical Chemistry, Justus-Liebig University Giessen, 35392 Giessen, Germany.

[b] Center for Materials Research (LaMa), Justus-Liebig University Giessen,35392 Giessen, Germany

[#] Corresponding author, Email: Doreen.Mollenhauer@phys.chemie.uni-giessen.de

S1: Frenkel pairs within 0D-, 1D- and 2.5D-LIPON

Table S1: Bounded and isolated (neutral and charged) Frenkel pair energies E_{FP} (eV) calculated in this study and taken from Ref. 1 and 2 (Ref. 1 marked with [*] and Ref. 2 marked with [+]) and the corresponding distances $d(\text{vac} - \text{int})$ (Å) between the Li vacancy positions and the Li interstitial positions of the bounded Frenkel pairs of the three LIPON structures for each Li vacancy positions are presented, using PBE-D3(BJ)/(PAW P) level of theory. The Frenkel pair energies E_{FP} (eV) calculated by means of the DFT approach fluctuate ($\tilde{U}_{max}$) by ± 4 % which represents a value of 0.05 eV for bounded pairs, as well as a value of 0.24 eV for neutral and 0.08 eV for charged isolated pairs. The preferred Frenkel pairs for each structure are highlighted in grey.

System	Frenkel pair vac	int	$E_{FP}(b)$ /eV (bound) and Ref. E_{FP} in brackets	$d(\text{vac} - \text{int})$ /Å	E_{FP} /eV neutral isolated	E_{FP} /eV charged isolated
0D	$V_1(6g)$	$I_1(2d)$	1.60 (>1.6[*])	3.58	4.92	0.99
	$V_1(6g)$	$I_2(1a)$	1.95 (>1.6[*])	6.35	5.32	1.22
	$V_1(6g)$	$I_3(3e)$	3.59	6.03	7.42	3.62
	$V_2(2c)$	$I_1(2d)$	0.86 (≈1.0[*])	4.10	5.18	1.32
	$V_2(2c)$	$I_2(1a)$	1.20 (≈1.0[*])	5.66	5.57	1.56
	$V_2(2c)$	$I_3(3e)$	2.82	3.51	7.67	3.95
	$V_3(6g')$	$I_1(2d)$	0.34 (0.3[*])	1.55	5.70	1.86
	$V_3(6g')$	$I_2(1a)$	1.18 (>1.0[*])	6.10	6.10	2.10
	$V_3(6g')$	$I_3(3e)$	2.79	5.70	8.19	4.49
1D	$V_1(8b)$	I_1	2.36 (≈2.0[+])	5.07	8.49	2.30
	$V_1(8b)$	I_2	2.55 (≈2.0[+])	3.94	8.69	2.51
2.5D	V_1	I_{G1}	0.32	2.72	4.49	0.39

V_1	I_{G2}	0.32	2.72	5.29	1.04
V_1	I_{G3}	-/-	-/-	6.05	1.42
V_2	I_{G1}	0.41	1.54	4.69	0.82
V_2	I_{G2}	0.53	2.72	5.49	1.47
V_2	I_{G3}	-/-	-/-	6.25	1.86
V_3	I_{G1}	0.75	2.75	4.75	0.87
V_3	I_{G2}	0.74	2.76	5.52	1.53
V_3	I_{G3}	1.5	4.28	6.28	1.91
V_4	I_{G1}	0.87	5.81	4.81	1.27
V_4	I_{G2}	0.84	5.54	5.61	1.93
V_4	I_{G3}	1.12	4.45	6.37	2.31
V_5	I_{G1}	0.43	4.79	5.41	1.68
V_5	I_{G2}	0.91	2.44	6.21	2.34
V_5	I_{G3}	-/-	-/-	6.96	2.72

As described in the main text, due to the pseudo-crystalline character of the 2.5D-LIPON structure, a large variety of different Li interstitial positions is possible. Due to local dissimilarities in the distance between the Li interstitial ion and neighboring nitrogen, oxygen, and phosphorus atoms, fluctuations in the formation energy occur in adjacent Li interstitial positions. To compensate these local dissimilarities, we grouped the Li interstitial positons into three groups based on their structural proximity to isolated PO_3^{4-} tetrahedra and PO_uN_{4-u} planes, see section 3a) and discussion in Section 3b). Therefore, only the energetically preferred Frenkel pairs within a Li interstitial positon group are listed in ESI Tab. S1 as well as in Tab. 4. However, we have characterized a variety of different bounded and isolated (both neutral and charged) Frenkel pairs within the 2.5D LIPON structure, see ESI Tab. S2.

Table S2: Listing of all identified bounded and isolated (neutral and charged) Frenkel pair energies E_{FP} (eV) within the 2.5D-LIPON structure, with the corresponding distances $d(vac - int)$ (Å) between the Li vacancy positions and the Li interstitial positions of the bounded Frenkel pairs, using PBE-D3(BJ)/(PAW P) level of theory. The Frenkel pair energies E_{FP} (eV) calculated by means of the DFT approach fluctuate ($\tilde{U}_{max}$) by ± 4 % which represents a value of 0.05 eV for bounded pairs, as well as a value of 0.24 eV for neutral and 0.08 eV for charged isolated pairs.

System	Frenkel pair		$E_{FP}(b)$ /eV bound	$d(vac - int)$ /Å	E_{FP} /eV neutral isolated	E_{FP} /eV charged isolated
	vac	int				
	V_1	I_{G1}	0.42	1.62	4.33	0.39
	V_1	I_{G1}	1.14	4.92	4.43	0.42
	V_1	I_{G1}	0.32	2.72	4.72	0.35
	V_1	I_{G2}	0.6	1.5	4.92	0.97
	V_1	I_{G2}	0.45	3.03	5.13	1.12
	V_1	I_{G2}	0.32	2.72	5.83	0.97
	V_1	I_{G3}	-/-	-/-	6.05	1.42
	V_2	I_{G1}	1.75	5.31	4.52	0.83
	V_2	I_{G1}	0.41	1.54	4.63	0.85
2.5D	V_2	I_{G1}	0.72	6.45	4.92	0.78
	V_2	I_{G2}	1.07	5.1	5.12	1.40
	V_2	I_{G2}	0.53	2.74	5.33	1.55
	V_2	I_{G2}	0.62	5.11	6.03	1.40
	V_2	I_{G3}	-/-	-/-	6.25	1.86
	V_3	I_{G1}	1.96	5.23	4.56	0.88
	V_3	I_{G1}	1.11	2.64	4.67	0.90
	V_3	I_{G1}	0.75	2.75	4.96	0.83
	V_3	I_{G2}	0.82	3.05	5.16	1.45
	V_3	I_{G2}	0.75	2.58	5.36	1.60

V_3	I_{G2}	0.74	2.76	6.06	1.45
V_3	I_{G3}	1.5	4.28	6.28	1.91
V_4	I_{G1}	2.35	5.41	4.64	1.28
V_4	I_{G1}	1.63	4.93	4.75	1.30
V_4	I_{G1}	0.87	5.81	5.04	1.23
V_4	I_{G2}	1.01	1.58	5.24	1.85
V_4	I_{G2}	0.84	5.45	5.44	2.00
V_4	I_{G2}	1	6.51	6.14	1.85
V_4	I_{G3}	1.12	4.45	6.37	2.31
V_5	I_{G1}	2.33	5.04	5.24	1.69
V_5	I_{G1}	0.43	4.79	5.35	1.72
V_5	I_{G1}	-/-	-/-	5.64	1.65
V_5	I_{G2}	1.92	5.61	5.84	2.27
V_5	I_{G2}	1.17	3.86	6.04	2.41
V_5	I_{G2}	0.91	2.44	6.74	2.26
V_5	I_{G3}	-/-	-/-	6.96	2.72

S2: Li vacancy diffusion paths within 0D-, 1D- and 2.5D-LIPON

Table S3: Li vacancies diffusion paths are presented with their migration energies $E_{mig,vac}$ (eV) for neutral and charges Li vacancies as well as the corresponding values from Ref. 1–3 (Ref. 1 marked with [*] and Ref. 2 marked with [+] and Ref. 3 marked with [#]), the number of steps per diffusion path (Σ steps) and the average distance between initial and final state d_{i-f} (Å) for the three LIPON structures, using PBE-D3(BJ)/(PAW P) level of theory. The Li vacancy migration energies $E_{mig,vac}$ calculated by means of the DFT approach fluctuate ($\tilde{U}_{max}$) by a value of 0.02 eV for neutral[4] and by ± 4 % which represents a value of 0.03 eV for charged Li vacancies. The preferred Li vacancy diffusion paths are highlighted in grey.

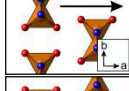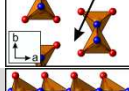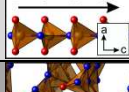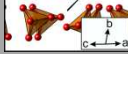| System	Path name	Li vacancy diffusion path[o]		neutral $E_{mig,vac}$ /eV	charged $E_{mig,vac}$ /eV	Ref. $E_{mig,vac}$ /eV	Σ steps	average d_{i-f}/Å
0D	p(6g↔6g (1))≈		within ab plane	0.36	0.38	- / 0.4[*]	5	2.66
	p(6g↔6g (2))≈			0.42	0.47	- / 0.3[*]	4	2.36
	p(6g↔6g (3))≈			0.42	0.47	- / -	2	2.38
	p(6g↔6g (4))≈			0.42	0.47	- / -	5	2.71
	p(6g'↔6g' (1))≈		within ab plane	0.41	0.47	- / 0.6[*]	4	2.52
	p(6g'↔6g' (2))≈			0.41	0.47	- / 0.6[*]	3	2.48
	p(6g'↔6g' (3))≈			0.57	0.64	- / 0.6[*]	4	2.41
	p(6g'↔6g' (4))≈			1.52	1.66	- / 1.6[*]	3	2.86
	p(2c↔2c)		within ab plane	1.86	2.03	- / -	1	5.58
	p(6g'↔2c↔6g)		6g'↔2c - along c-axis	0.08 / 0.60[‡]	0.13 / 0.67[‡]	- / -	1	2.29
			2c↔6g - along c-axis	0.05 / 0.30[‡]	0.09 / 0.42[‡]	- / -	1	2.25
1D	p(a)		parallel a-axis	0.61	0.64	~0.55[+] / -	2	2.97
	p(b (1))≈		parallel b-axis	0.61	0.64	~0.6[+] / -	2	2.99
	p(b (2))≈			0.61	0.64	~0.6[+] / -	1	3.08
	p(c (1))≈		parallel c-axis	0.40	0.49	~0.45[+] / -	2	2.90
	p(c (2))≈			1.61	1.71	- / -	2	4.35
2.5D	p(I (1))≈		within ac plane	0.45	0.55	- / -	2	3.03
	p(I (2))≈			0.57	0.69	- / -	2	2.95
	p(I (3))≈			1.37	1.38	- / -	1	4.15
	p(I (4))≈			1.56	1.57	- / -	1	4.15
	p(II (1))≈		within ac plane	0.45	0.67	- / -	2	2.90
	p(II (2))≈			0.57	0.69	- / -	2	2.89
	p(III)		within ac plane	0.46	0.63	- / 0.53[#]	2	3.09
	p(b)		parallel b-axis	>5	>5	- / -	1	5.58
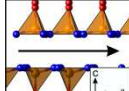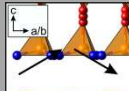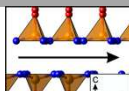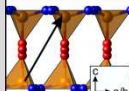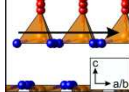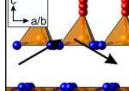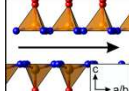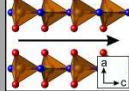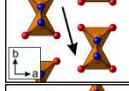
[≈] multiple energetical equal diffusion paths are possible within this orientation

[‡] migration energy of initial to final state is not equal to that of final to initial state (directional dependency)

[o] black arrow illustrates the diffusion direction or orientation

S3: Li interstitial diffusion paths within 0D-, 1D- and 2.5D-LIPON

Table S4: Charged Li interstitial diffusion paths are presented with their migration energies $E_{\text{mig,int}}$ (eV) for the direct and indirect process as well as the corresponding values from Ref. 1–3 (Ref. 1 marked with [*] and Ref. 2 marked with [+] and Ref. 3 marked with [#]) and the average distance between initial and final state $d_{\text{i-f}}$ (Å) for the three LIPON structures, using PBE-D3(BJ)/ (PAW P) level of theory. The charged Li interstitial migration energies $E_{\text{mig,int}}$ calculated by means of the DFT approach fluctuate ($\tilde{U}_{\text{max}}$) by ± 4 % which represents a value of 0.04 eV for the direct and 0.03 eV for the indirect diffusion. The preferred direct charged Li interstitial diffusion paths are highlighted in light grey and indirect in dark grey.

System	Path classification	Li interstitial diffusion path[o]	direct $E_{\text{mig,int}}$ /eV and Ref. $E_{\text{mig,int}}$ in brackets	indirect $E_{\text{mig,int}}$ /eV and Ref. $E_{\text{mig,int}}$ in brackets	average $d_{\text{i-f}}$ /Å
0D	p(I$_2$(1a)↔I$_2$(1a))$^{≈,bg}$		along a- or b axis or within ab plane	1.72^{bg}	-/-	5.56
	p(I$_2$(1a)↔I$_1$(2d))$^{≈}$		along a or b-axis +1/4c or within ab plane +1/4c	> 2.0 (> 2.0[*])	0.45 / 0.68‡ (~0.45 / 0.6‡[*])	3.82
	p(I$_2$(1a)↔I$_3$(3e))$^{≈}$		along a- or b axis or within ab plane	> 2.0	2.40	2.74
	p(I$_1$(2d)↔I$_1$(2d) (c))		parallel c-axis	1.38	1.20	5.24
	p(I$_1$(2d)↔I$_1$(2d) (a/b))		along a- or b axis or within ab plane	-/-	-/-	5.58
	p(I$_1$(2d)↔I$_3$(3e))$^{≈}$		along a or b-axis +1/4c or within ab plane +1/4c	2.66	>3.0	2.67
	p(I$_3$(3e)↔I$_3$(3e))$^{≈}$		along a- or b axis or within ab plane	-/-	-/-	4.82
1D	p(I$_1$↔I$_1$ (c))		parallel c-axis	1.02 (≈0.95[+])	0.60	2.34
	p(I$_1$↔I$_1$ (b))		parallel b-axis	-/-	>1.1	2.76
	p(I$_1$↔I$_2$ (a))		parallel a-axis	0.86 / 0.64‡ (≈0.75 / ≈0.55‡[+])	0.62 / 0.40‡	2.50
	p(I$_1$↔I$_2$ (b))		parallel b-axis	-/-	0.71 / 0.49‡	3.13
	p(I$_2$↔I$_2$ (c))		parallel c-axis	0.68 (≈0.65[+])	-/-	2.46
2.5D	p(I$_{G1}$↔I$_{G1}$ (ac))		within ac plane	-/-(0.65[#])	0.46	4.13

System	Path classification	Li interstitial diffusion path[o]	direct $E_{mig,int}$ /eV and Ref. $E_{mig,int}$ in brackets	indirect $E_{mig,int}$ /eV and Ref. $E_{mig,int}$ in brackets	average d_{i-f} /Å
	p(I$_{G3}$↔I$_{G2}$ (b))		0.38 / 0.08 [‡]	-/-	2.28
	p(I$_{G1}$↔I$_{G1}$ (ac))[bg]		>2[bg]	-/-	8.14
	p(I$_{G1}$↔I$_{G2}$ (ac))[bg]		>0.6[bg]	-/-	4.64

[≈] orientation of Li interstitial diffusion has no influence on the migration energy and can take place either along the *a*- or *b*-axis, see SI Fig. S2
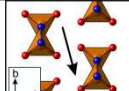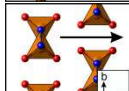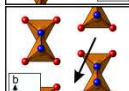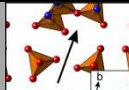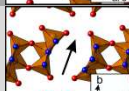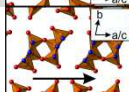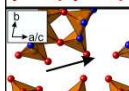
[‡] migration energy of initial to final state is not equal to that of final to initial state (directional dependency)

[o] black arrow illustrates the diffusion direction or orientation

[bg] in addition to the Li interstitial ion or indirect Li ion other Li ions are migrating around their position in the supercell. In this case a *background diffusion* occurs.

Table S5: Neutral Li interstitial diffusion paths are presented with their migration energies $E_{mig,int}$ (eV) for the direct and indirect process as well as the corresponding values from Ref. 1–3 (Ref. 1 marked with [*] and Ref. 2 marked with [+] and Ref. 3 marked with [#]) and the average distance between initial and final state d_{i-f} (Å) for the three LIPON structures, using PBE-D3(BJ)/ (PAW P) level of theory. The neutral Li interstitial migration energies $E_{mig,int}$ calculated by means of the DFT approach fluctuate (Ŭ$_{max}$) by ±4 % which represents a value of 0.04 eV for the direct and 0.03 eV for the indirect diffusion. The preferred direct neutral Li interstitial diffusion paths are highlighted in light grey and indirect in dark grey.

System	Path classification	Li interstitial diffusion path[o]	direct $E_{mig,int}$ /eV and Ref. $E_{mig,int}$ in brackets	indirect $E_{mig,int}$ /eV and Ref. $E_{mig,int}$ in brackets	average d_{i-f} /Å
	p(I$_2$(1a)↔I$_2$(1a))[≈ bg]		along *a*- or *b* axis or within *ab* plane	1.35[bg]	-/-	5.59
	p(I$_2$(1a)↔I$_1$(2d))[≈]		along *a* or *b*-axis +1/4c or within *ab* plane +1/4c	> 2.0	0.27 / 0.67[‡]	3.61
	p(I$_2$(1a)↔I$_3$(3e))[≈]		along *a*- or *b* axis or within *ab* plane	> 2.0	2.10	2.83
0D	p(I$_1$(2d)↔I$_1$(2d) (c))		parallel *c*-axis	1.45	1.25	5.16
	p(I$_1$(2d)↔I$_1$(2d) (a/b))		along *a*- or *b* axis or within *ab* plane	-/-	-/-	5.66
	p(I$_1$(2d)↔I$_3$(3e))[≈]		along *a* or *b*-axis +1/4c or within *ab* plane +1/4c	2.50	>3.0	2.78
	p(I$_3$(3e)↔I$_3$(3e))[≈]		along *a*- or *b* axis or within *ab* plane	-/-	-/-	4.86

Note: The second table has an extra "Li interstitial diffusion path" description column merged with the path image column.

| System	Path classification	Li interstitial diffusion path[o]		direct $E_{mig,int}$ /eV and Ref. $E_{mig,int}$ in brackets	indirect $E_{mig,int}$ /eV and Ref. $E_{mig,int}$ in brackets	average d_{i-f} /Å
1D	p($I_1 \leftrightarrow I_1$ (c))		parallel c-axis	0.80	0.44	2.11
	p($I_1 \leftrightarrow I_1$ (b))		parallel b-axis	-/-	>1.1	2.67
	p($I_1 \leftrightarrow I_2$ (a))		parallel a-axis	0.59 / 0.42[‡]	0.45 / 0.32[‡]	2.53
	p($I_1 \leftrightarrow I_2$ (b))		parallel b-axis	-/-	0.56 / 0.38[‡]	3.15
	p($I_2 \leftrightarrow I_2$ (c))		parallel c-axis	0.53	-/-	2.88
2.5D	p($I_{G1} \leftrightarrow I_{G1}$ (b))		parallel b-axis	-/-	0.06 / 0.34[‡]	4.81
	p($I_{G3} \leftrightarrow I_{G2}$ (b))		parallel b-axis	0.91	-/-	2.39
	p($I_{G1} \leftrightarrow I_{G1}$ (ac))[bg]		within ac plane	>2.0[bg]	-/-	8.15
	p($I_{G1} \leftrightarrow I_{G2}$ (ac))[bg]		within ac plane	>1.3[bg]	-/-	4.65

≈ orientation of Li interstitial diffusion has no influence on the migration energy and can take place either along the *a*- or *b*-axis, see SI Fig. S2

‡ migration energy of initial to final state is not equal to that of final to initial state (directional dependency)

o black arrow illustrates the diffusion direction or orientation

bg in addition to the Li interstitial ion or indirect Li ion other Li ions are migrating around their position in the supercell. In this case a *background diffusion* occurs.

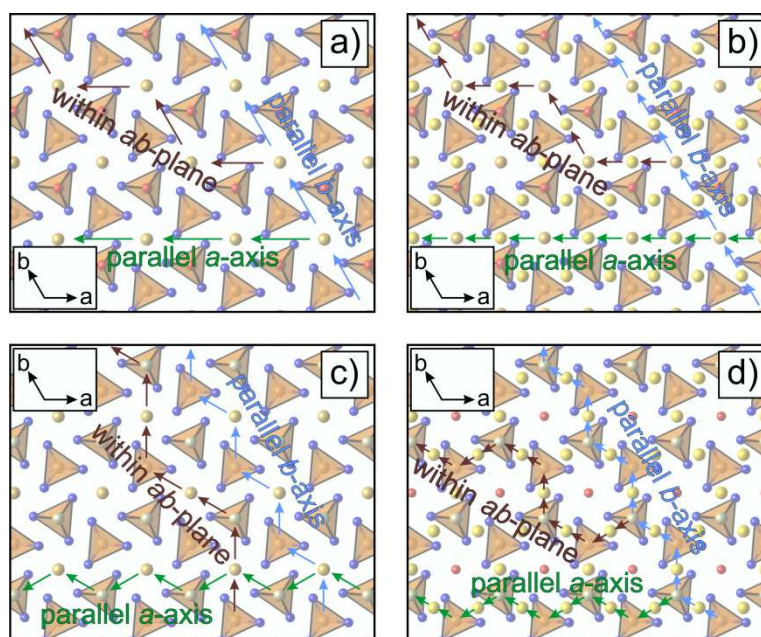## S4: Li interstitial diffusion paths within 0D-LIPON
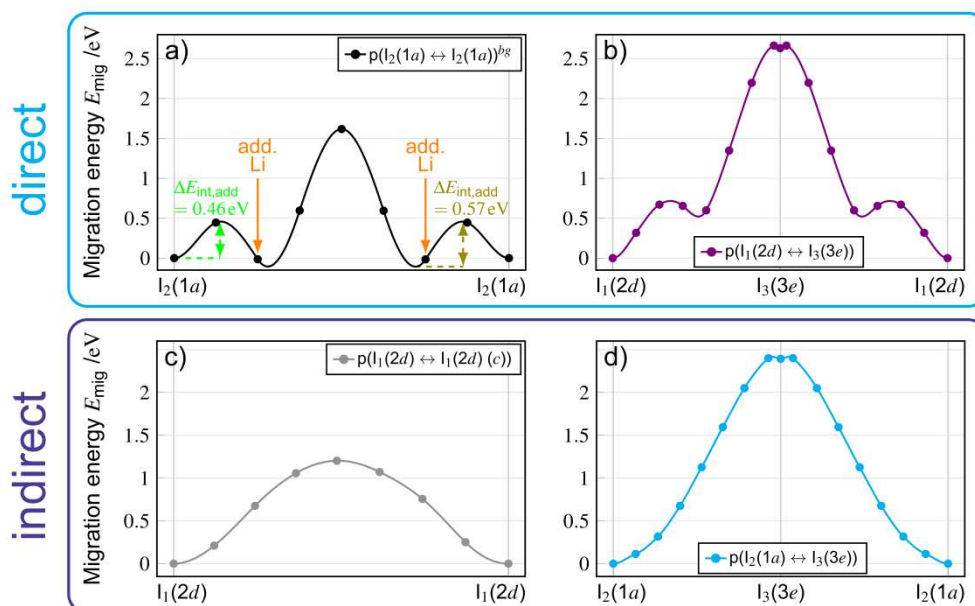
Figure S1: Energetics of the charged Li interstitial direct [a) and b)] and indirect [c) and d)] diffusion paths within the 0D-LIPON structure. a) $p(I_2(1a)\leftrightarrow I_2(1a))^{bg}$ direct (^{bg} marks a occurring *background diffusion*), b) $p(I_1(2d)\leftrightarrow I_3(3e))$ direct, c) $p(I_1(2d\leftrightarrow I_1(2d)\,(c))$ indirect and d) $p(I_2(1a)\leftrightarrow I3(3e))$ indirect. Orange arrows in a): Influence of the additionally migrating Li ions on the energetic diffusion path.
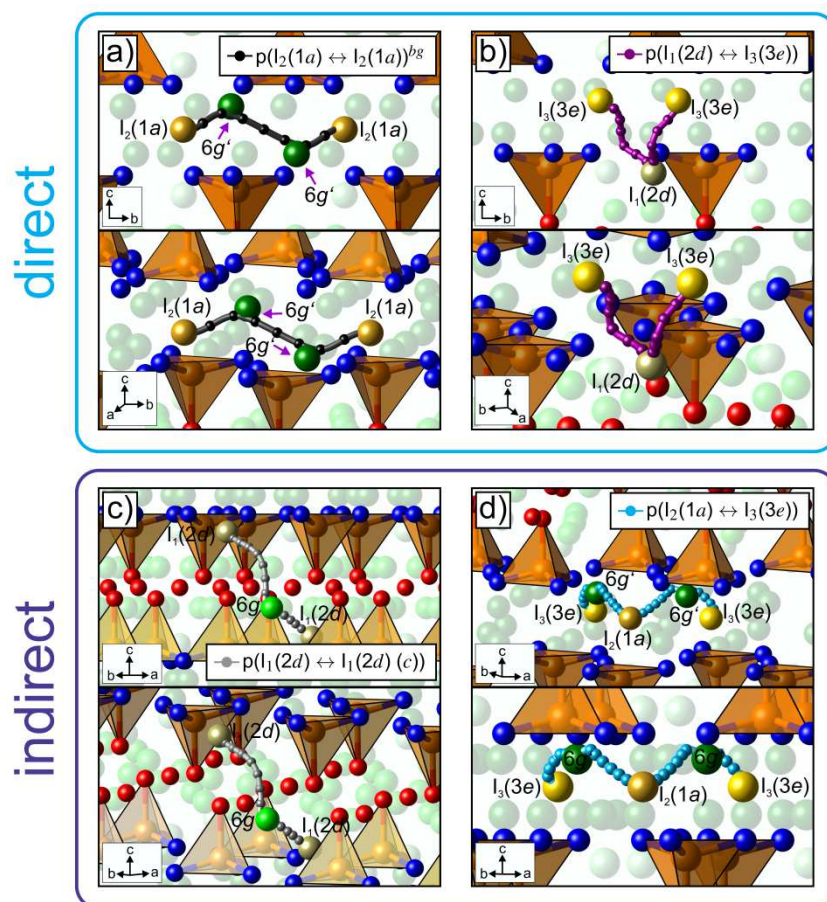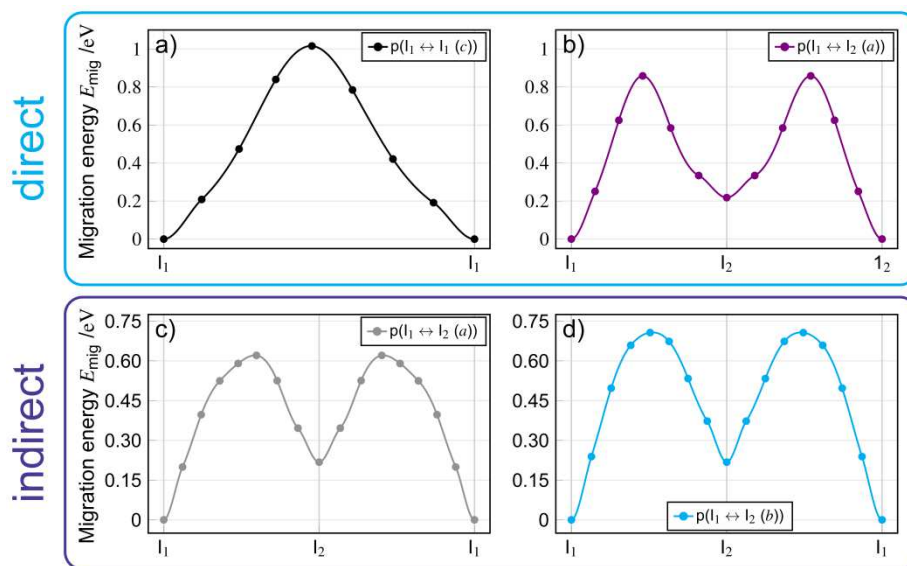
Figure S2: Structural visualization (above: overview and below: detailed view) of the charged Li interstitial direct [a) and b)] and indirect [c) and d)] diffusion paths within the 0D-LIPON structure. The paths correspond to Fig. S1. Color Code: orange: phosphorous, red: oxygen; blue: nitrogen, green: lithium at $6g$ positions, dark green: lithium at $6g'$ positions, light green: lithium at $2c$ positions, ochre: Li interstitial at $I_1(2d)$ positions, gold: Li- interstitial at $I_2(1a)$ positions and dark yellow: Li-interstitial at $I_3(3e)$ positions. Violet arrows in a): emphasizing the additional migrating lithium ions in the structural diffusion path. [bg] in a) marks a occurring *background diffusion*.

Figure S3: Orientations of the Li interstitial (direct as well as indirect) diffusion within the 0D-LIPON structure. a) $p(I_2(1a) \leftrightarrow I_2(1a))$, b) $p(I_2(1a) \leftrightarrow I_3(3e))$, c) $p(I_2(1a) \leftrightarrow I_1(2d))$ and $p(I_1(2d) \leftrightarrow I_3(3e))$ diffusion. Color code: orange: phosphorous, red: oxygen, blue: nitrogen, ochre: Li interstitial at $I_1(2d)$ positions, gold: Li interstitial at $I_2(1a)$ positions and dark yellow: Li interstitial at $I_3(3e)$ positions. Green arrows represent the diffusion parallel to the a-axis, blue arrows parallel to the b-axis and dark red arrows within the ab plane.

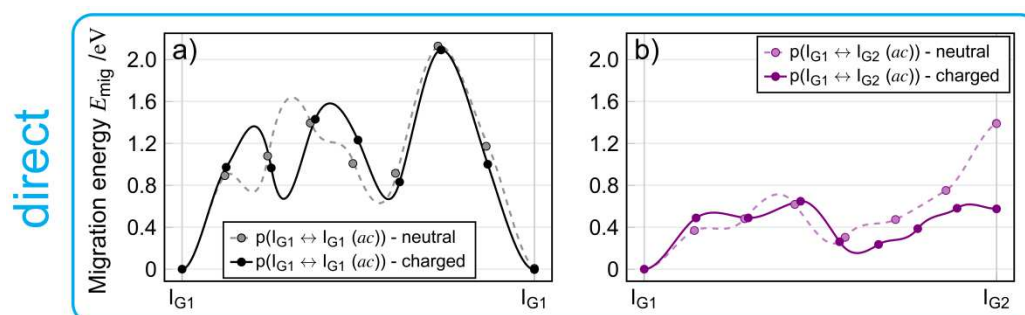## S5: Li interstitial diffusion paths within 1D-LIPON

Figure S4: Energetics of the charged Li interstitial direct [a) and b)] and indirect [c) and d)] diffusion paths within the 1D-LIPON structure. a) $p(I_1 \leftrightarrow I_1 (c))$ direct, b) $p(I_1 \leftrightarrow I_2 (a))$ direct, c) $p(I_1 \leftrightarrow I_2 (a))$ indirect and d) $p(I_1 \leftrightarrow I_2 (b))$ indirect.
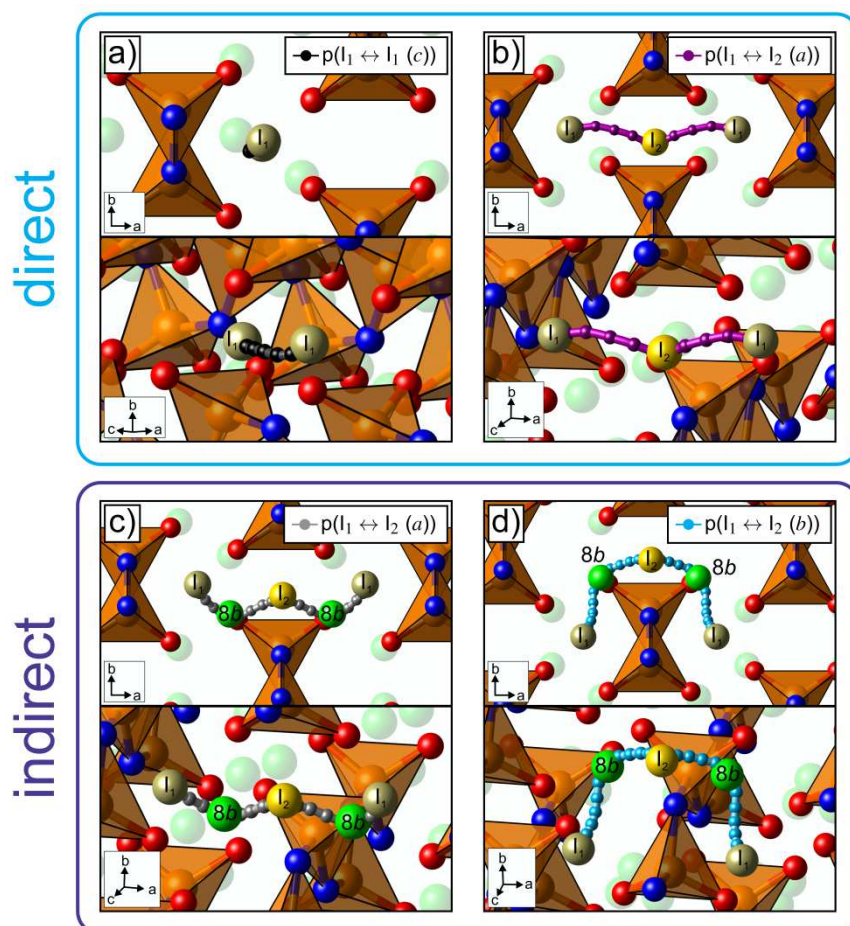
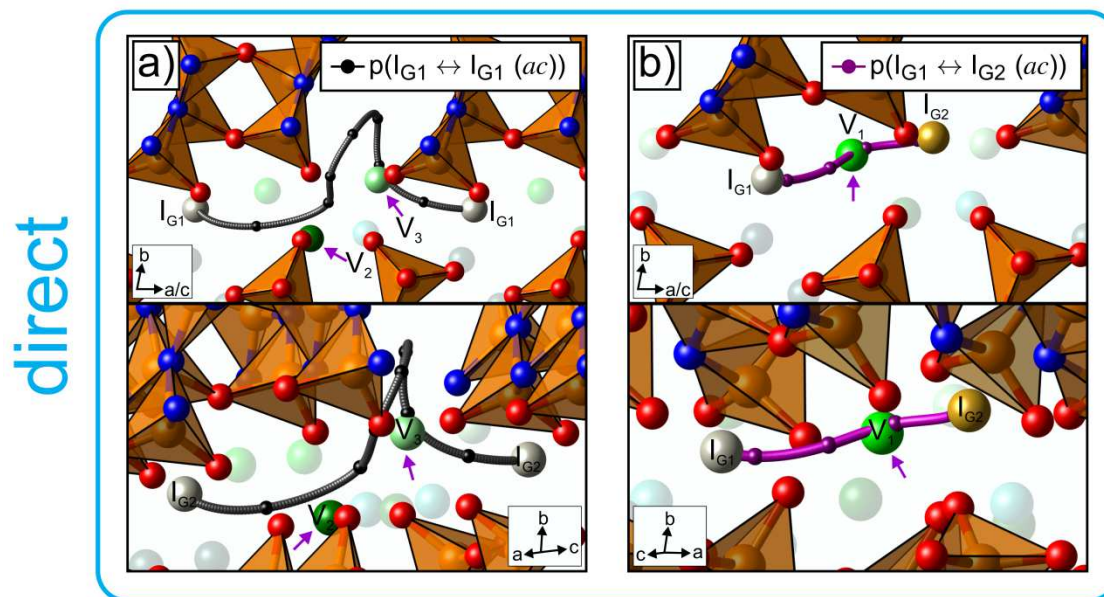**Figure S5:** Structural visualization (above: overview and below: detailed view) of the charged Li interstitial direct [a) and b)] and indirect [c) and d)] diffusion paths within the 1D-LIPON structure. The paths correspond to Fig. S4. Color Code: orange: phosphorous, red: oxygen, blue: nitrogen, green: lithium at $8b$ positions, ochre: Li interstitial at I_1 positions and dark yellow: Li interstitial at I_2 positions.

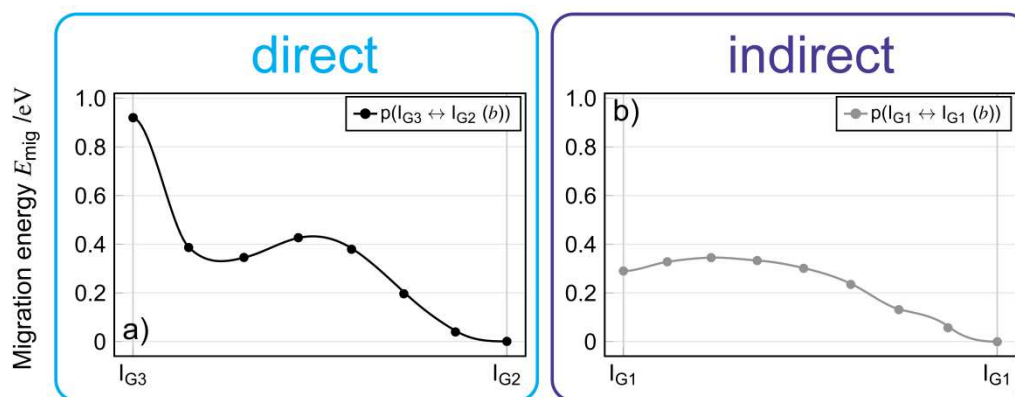## S6: Li interstitial diffusion paths within 2.5D-LIPON

Examples of the increased *background diffusion* during charged and neutral Li interstitial diffusion within the 2.5D-LIPON structure are the direct paths p($I_{G1}\leftrightarrow I_{G1}$ (ac)) and p($I_{G1}\leftrightarrow I_{G2}$ (ac)) which both take place in the *ac* plane and are shown in Figs. S6 and S7. Within the $I_{G1}\leftrightarrow I_{G1}$ diffusion path two other Li ions (marked as light green and dark green Li ions) move parallel to the interstitial ion. One Li ion (dark green) returns to its equilibrium position after it provided space for the passing interstitial Li ion, analogous to the 0D-structure of the p($I_2(1a)\leftrightarrow I_2(1a)$) path. However, the second Li ion (light green) moves to a new location during the Li interstitial diffusion process and remain there, although the migration interstitial Li ion has passed by. During the p($I_{G1}\leftrightarrow I_{G2}$ (ac))diffusion path only one additional Li ion moves, which provides space for the interstitial Li ion and returns afterwards to its equilibrium position. Furthermore, the obtained migration energy for the paths p($I_{G1}\leftrightarrow I_{G1}$ (ac)) as well as for the p($I_{G1}\leftrightarrow I_{G2}$ (ac))diffusion path is above 0.5 eV (see ESI Tab. S4 for charged and S5 for neutral), but the reliability of these energies cannot final be determined.


Figure S6: Energetics of the charged (solid line) and neutral (dashed line) Li interstitial direct [a) and b)] diffusion paths within the 2.5D-LIPON structure. a) p($I_{G1}\leftrightarrow I_{G1}$ (ac))direct, b) p($I_{G1}\leftrightarrow I_{G2}$ (ac)) direct.

Figure S7: Structural visualization (above: overview and below: detailed view) of the Li interstitial direct [a) and b)] diffusion paths within the 2.5D-LIPON structure. The paths correspond to Fig. S6. Color Code: orange: phosphorous, red: oxygen, blue: nitrogen, green: lithium at V_1 positions, dark green: lithium at V_2 positions, light green: lithium at V_3 positions, turquoise: lithium at V_4 positions, dark turquoise: lithium at V_5 positions, ochre: Li interstitial at I_{G1} positions, gold: Li interstitial at I_{G2} positions and dark yellow: Li interstitial at I_{G3} positions. Violet arrows in a): emphasizing the additional migrating lithium ions in the structural diffusion path.

Figure S8: Energetics of the neutral Li interstitial direct [a)] and indirect [b)] diffusion paths within the 2.5D-LIPON structure. a) p($I_{G3} \leftrightarrow I_{G2}$ (b))direct, b) p($I_{G1} \leftrightarrow I_{G1}$ (b)) indirect.
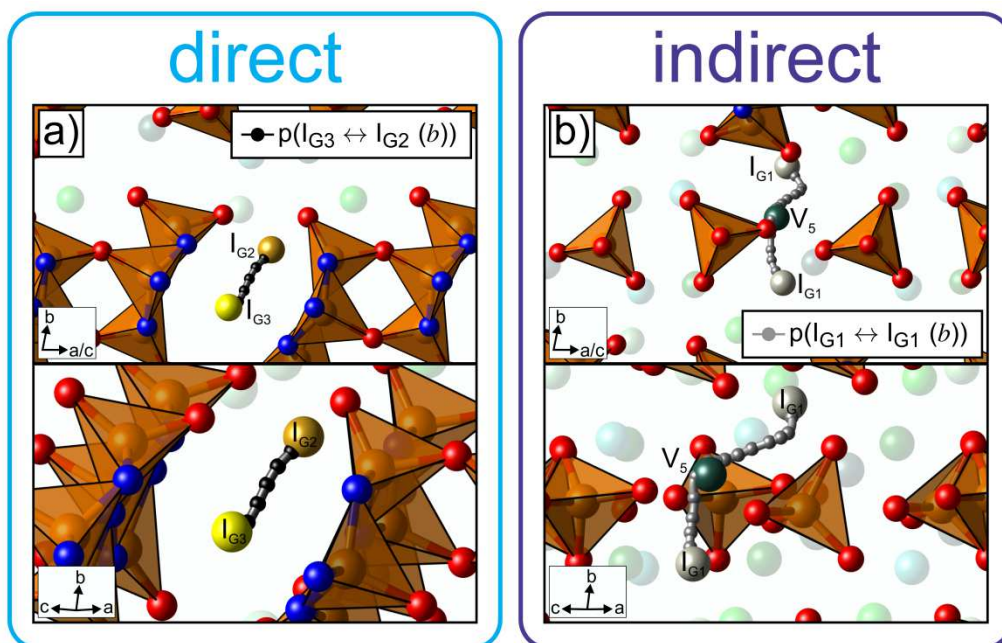
Figure S9: Structural visualization (above: overview and below: detailed view) of the Li interstitial direct [a) and b)] diffusion paths within the 1D-LIPON structure. The paths correspond to Fig. S8. Color Code: orange: phosphorous, red: oxygen, blue: nitrogen, green: lithium at V_1 positions, dark green: lithium at V_2 positions, light green: lithium at V_3 positions, turquoise: lithium at V_4 positions, dark turquoise: lithium at V_5 positions, ochre: Li interstitial at I_{G1} positions, gold: Li interstitial at I_{G2} positions and dark yellow: Li interstitial at I_{G3} positions. Violet arrows in a): emphasizing the additional migrating lithium ions in the structural diffusion path.

S7: Frenkel pair $x_{\mathrm{FP}}(T)$ and free carrier concentration $n(T)$ for 0D-, 1D- and 2.5D-LIPON

Table S6: Frenkel pair concentration $x_{\mathrm{FP}}(T)$ and free carrier concentration $n(T)$ of charged and neutral Li vacancies and Li interstitials for the three LIPON structures at RT (T = 298°K), using PBE-D3(BJ)/(PAW P) level of theory. Based on the ± 4 % fluctuation range, the uncertainties of the calculated values of $x_{\mathrm{FP}}(T)$ and $n(T)$ are determined.

System	charge state	$x_{\mathrm{FP}}(T)^{\pm}$	$n(T)^{\pm}$ /mol/cm^3
0D	charged	$(1.34 \pm 0.05) \cdot 10^{-3}$	$(1.05 \pm 0.04) \cdot 10^{-5}$
	neutral		
1D	charged*	$(3.64 \pm 0.15) \cdot 10^{-20}$	$(2.67 \pm 0.11) \cdot 10^{-23}$
	neutral*	$(1.13 \pm 0.05) \cdot 10^{-20}$	$(8.31 \pm 0.33) \cdot 10^{-23}$
2.5D	charged	$(1.97 \pm 0.08) \cdot 10^{-3}$	$(1.52 \pm 0.06) \cdot 10^{-5}$
	neutral		

$\pm$ = Uncertainties for $x_{\mathrm{FP}}(T)$ and $n(T)$ are computed by assuming a ± 4 % fluctuation

* for charged species, the isolated Frenkel pair energy E_{FP} is slightly energetically favored compared to the bound energy, whereas for neutral species it is *vice versa*, see Tab. 4

References

(1) Al-Qawasmeh, A.; Holzwarth, N.A.W. $Li_{14}P_2O_3N_6$ and Li_7PN_4 : Computational study of two nitrogen rich crystalline LiPON electrolyte materials. *J. Power Sources* **2017**, *364*, 410–419.

(2) Senevirathne, K.; Day, C. S.; Gross, M. D.; Lachgar, A.; Holzwarth, N.A.W. A new crystalline LiPON electrolyte: Synthesis, properties, and electronic structure. *Solid State Ion.* **2013**, *233*, 95–101.

(3) Sicolo, S.; Albe, K. First-principles calculations on structure and properties of amorphous $Li_5P_4O_8N_3$ (LiPON). *J. Power Sources* **2016**, *331*, 382–390.

(4) Henkel, P.; Mollenhauer, D. Uncertainty of exchange-correlation functionals in density functional theory calculations for lithium-based solid electrolytes on the case study of lithium phosphorus oxynitride. *J. Comput. Chem.* **2021**, *42*, 1283–1295.